Chapter 2

Overview of DIS Experiments and Parameterizations

This chapter provides a general overview about the lepton deep inelastic scattering measurements which have enriched our phenomenological analysis performed in this thesis. Specifically the experimental results for non-singlet structure functions and associated sum rules for both polarized and unpolarized cases measured in electron, muon and neutrino DIS are reviewed. In addition, several parametrization associated with the determination of non-singlet structure functions are discussed.

2.1 Introduction

Particle Physics is a subject that can only thrive when there is a coherent interplay between theory and experiment. New theoretical ideas lead to predictions that can be tested experimentally, and new experimental findings challenge theorists to develop better ideas. Phenomenology is research on this boundary between theory and experiment. It is concerned with exploration of interesting physical observables, making theoretical predictions for them and then confronting experimental data gathered at the major international experimental laboratories. The primary goal of phenomenology is to find experimental evidences for new physics and to develop new theories that describe the Universe at a more fundamental level than our current theories can.

The work presented in this thesis is basically a phenomenological analysis of the non-singlet structure functions and the sum rules associated with them, along with higher order perturbative QCD and non-perturbative effects. This phenomenological analysis is enriched by several experimental results, along with a large numbers of

Experiment	Beam	Target	x	Q^2 (GeV^2)	Energy (GeV)	Ref.
NMC	μ	p, d	0.008 - 0.5	0.8 - 65	90, 120 200, 280	[63]
CCFR	$\nu_\mu(\bar{\nu}_\mu)$	Fe	0.015 - 0.65	1.2 - 126	30 - 500	[66]
NuTeV	$\nu_\mu(\bar{\nu}_\mu)$	Fe	0.015 - 0.75	1.2 - 125	30 - 360	[68]
CHORUS	$\nu_\mu(\bar{\nu}_\mu)$	Pb	0.02 - 0.65	0.3 - 82	30 - 360	[70]
SLAC(E143)	e^-	NH_3, ND_3	0.03 - 0.5	1 - 10	≤ 28	[75]
SMC	μ^+	H/D-butanol NH_3	0.004 - 0.5	1 - 60	100, 190	[74]
HERMES	e^-,e^+	H, D, ^{3}He	0.02 - 0.7	1 - 15	27.5	[73]
COMPASS	μ^+	NH_3,^{6}LiD	0.003 - 0.6	1 - 70	160	[71]
JLAB (Hall A)	e^-	^{3}He	0.1 - 0.6	1 - 2.5	6	[72]
JLAB (Hall B)	e^-	NH_3, ND_3	0.05-0.6	1 - 5	≤ 6	[95]

Table 2.1: Table of datasets used in the phenomenological analysis of this thesis. The kinematic range of each measurement in x and Q^2 and the incident beam energy are also given.

parameterizations. A brief description of different experiments and parameterizations, their results for non-singlet structure functions and associated sum rules is given in this chapter.

2.2 DIS Experiments and Results

Many successful experimental programs of both unpolarized and Polarized deep inelastic lepton scattering experiments have been carried out at SLAC, CERN, Fermilab, DESY and Jefferson Laboratory(JLab)(See for more details [59–62]) in order to elucidate the internal structure of the nucleon. With the advent of dedicated experimental facilities, recent experiments were able to determine the structure functions as well as different sum rules over a wide range of x and Q^2 with ever increasing precision.

We have summarized different DIS experiments that have probed the nucleon structure in Table 2.1 along with the x, Q^2 ranges and beam energies of the measurements. However, as our works deal with the non-singlet structure functions and the kinematical region of our consideration is $x \leq 0.05$ and $1.3 \leq Q^2 \leq 20$, we shall restrict our discussion on the following unpolarized DIS experiments: NMC[63–65], CCFR[66, 67], NuTeV[68], CDHSW[69] and CHORUS[70] experiments which are

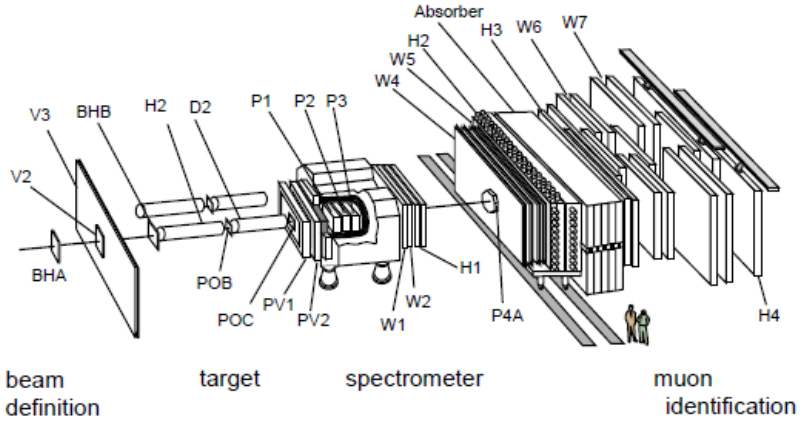

Figure 2.1: Schematic diagram of the NMC spectrometer.

associated with the measurements of the non-singlet structure functions F_2^{NS} and xF_3 and the sum rules Gottfried Sum rule(GSR)[34, 35] and Gross-Llewellyn Smith Sum Rule(GLSSR)[38, 39] and polarized experiments: COMPASS[71], HERMES[73], SMC[74], E143[75] and JLab experiments[76–78], which are associated with the measurements of non-singlet spin structure function g_1^{NS} and the Bjorken Sum rule[42,43], associated with g_1^{NS}.

2.2.1 NMC

The New Muon Collaboration(NMC) was constructed at CERN to study DIS using muon beams on proton and deuterium targets. It was an extension and improvement of the European Muon Collaboration(EMC) experiment. Aiming towards better measurements of nuclear effects in DIS, particularly the EMC effect, the NMC was designed. It has also designed to have accurate data on the structure functions F_2^p and F_2^d and to measure structure function ratios with high precision.

A schematic diagram of the NMC apparatus is shown in Fig. 2.1[79]. It is consisted of an upstream beam momentum station(BMS) and hodoscopes, a downstream beam calibration spectrometer(BCS), a target region and a muon spectrometer. The muon beam ran at beam energies of 90, 120, 200, and 280 GeV and illuminated two target cells containing liquid hydrogen and liquid deuterium placed in series along the beam axis. Since the spectrometer acceptance was very different for both targets they were regularly alternated. The muon spectrometer was surrounded by several MWPCs and drift chambers to allow a full reconstruction of the interaction vertex and the scattered muon trajectory. Muons were identified using drift chambers placed behind a thick iron absorber.

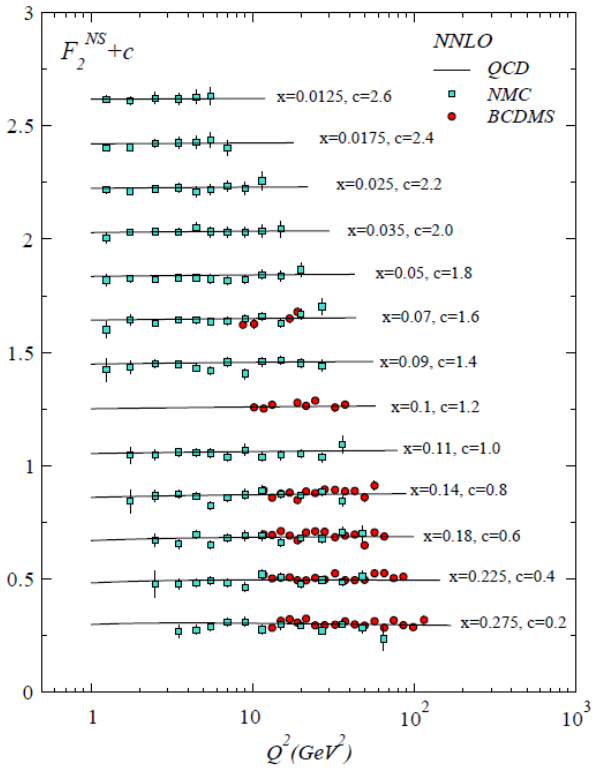

Figure 2.2: NMC measurements[63] of F_2^{NS} structure function along with BCDMS data. (Fig. taken from [80].)

The experiment published measurements of the proton and deuteron differential cross sections $d^2/dxdQ^2$ in the region $0.008 < x < 0.5$ and $0.8 < Q2 < 65GeV2$, from which the structure functions F_2^p and F_2^d were extracted[63]. The NMC data consist of four data sets for the proton and the deuteron structure functions corresponding to beam energies of 90 GeV, 120 GeV, 200 GeV, and 280 GeV. They cover the kinematic range $0.002 \leq x \leq 0.60$ and $0.5GeV^2 \leq Q^2 \leq 75GeV^2$.

In 1992 NMC published the first data on the Gottfried sum rule[64]. The initial NMC measurement indicated a violation of this assumption of a flavour symmetric sea. This was verified by the final NMC analysis[65] in which the Gottfried sum was determined to be 0.2350.026 at $Q2 = 4GeV2$, which implies that $\int dx(\bar{d} - \bar{u}) \sim 0.15$, indicating a significant excess of $\bar{d}$ over $\bar{u}$.

The experimental results for the non-singlet structure function, F_2^{NS} extracted from NMC measurements are taken from Ref. [63] and the results obtained in [63] are presented in Fig.2.2. Further the GSR results obtained in [65] are shown in Fig. 2.3.

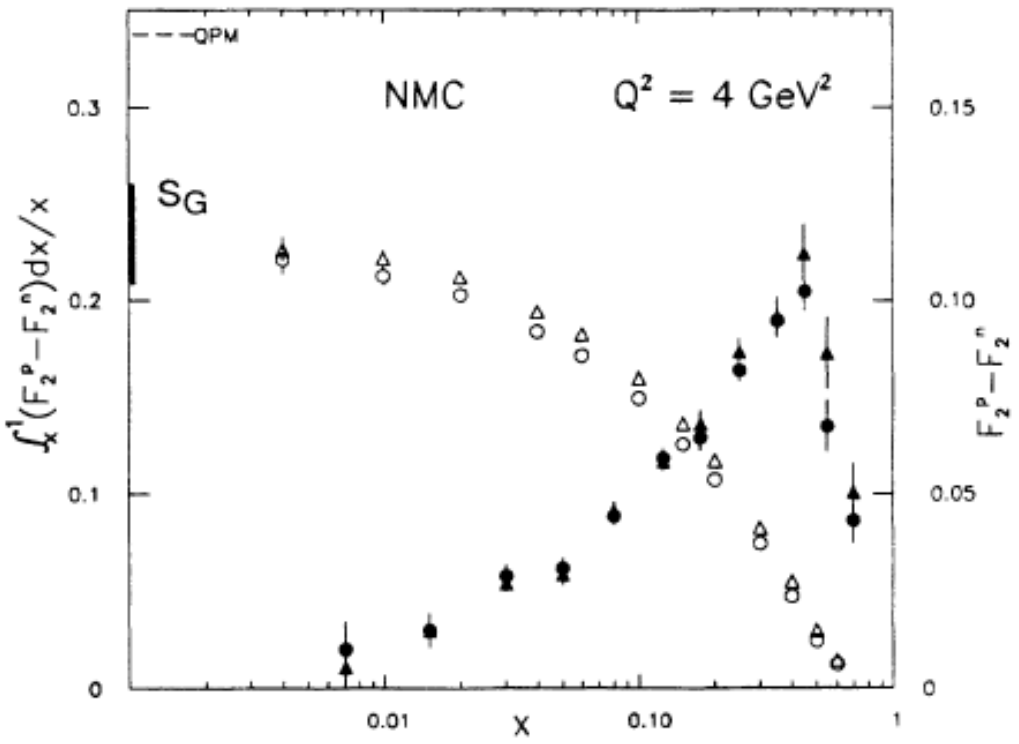

Figure 2.3: NMC measurements of Gottfried sum rule[65].

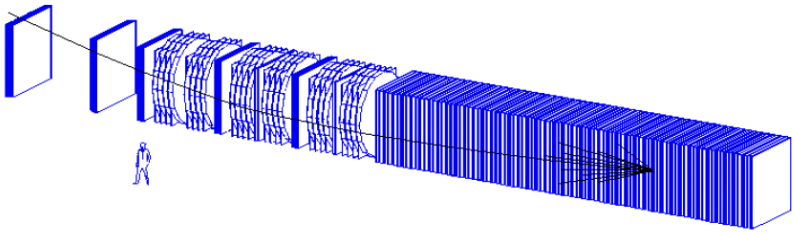

Figure 2.4: Schematic diagram of the CCFR Dtector.

2.2.2 CCFR

The Chicago-Columbia-Fermilab-Rochester detector (CCFR) was constructed at the Fermi National laboratory, Fermilab to study DIS in neutrino induced lepton beams on an almost isoscalar iron target.

The CCFR detector, shown in Fig. 2.4 uses a wide-band mixed neutrino (ν_μ) and antineutrino($\bar{\nu}_\mu$) beam with energies up to 600 GeV. The CCFR detector which was used to observe neutrino interactions consists of an iron based target-calorimeter instrumented with both scintillators and drift chambers and a toroid muon spectrometer. The neutrino DIS data were collected in two high energy high statistics runs, E744 and E770 in Fermilab By CCFR collaboration.

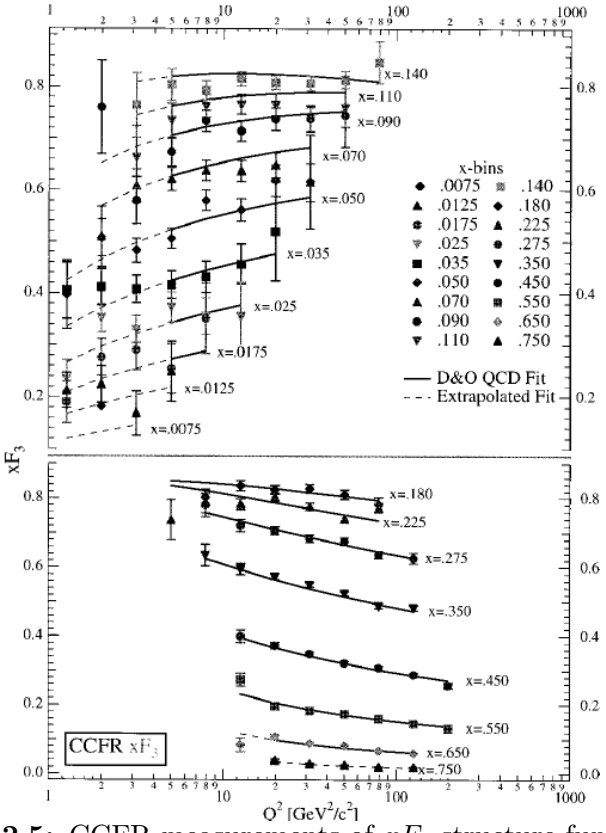

Figure 2.5: CCFR measurements of xF_3 structure function[66].

The non-singlet structure function, xF_3 extracted from the CCFR data is shown in Fig. 2.5. They are with very small systematic errors(which is shown by the corresponding error bars in the Fig. 2.5). In Figs. 2.6 and 2.7, the results for GLS sum rule obtained by CCFR collaboration[67] are shown. In order to perform phenomenological analysis in this thesis we have used these results for both xF_3 structure function and GLSSR.

2.2.3 NUTEV

NeUtrino experiment at the fermlab TeVatron(NuTeV) is a neutrino-iron DIS experiment(E815) that collected separate high statistics neutrino and antineutrino data in 1996-97 at Fermilab. NuTeV's detector(Similar to CCFR, Fig. 2.4)(see [81] for details) consists of an iron target calorimeter (upstream) and a toroid muon spectrometer (downstream). The target calorimeter is an instrumented iron-scintillator sandwich interspersed with drift chambers. The measured hadronic shower energy resolution is $\frac{\sigma_E}{E} = \frac{0.89}{\sqrt{E}} \bigoplus 0.021$. The toroid spectrometer is constructed of steel washers and five drift chambers. Muon energy resolution is limited by multiple Coulomb scattering to $\frac{\sigma_p}{p} = 0.11$.

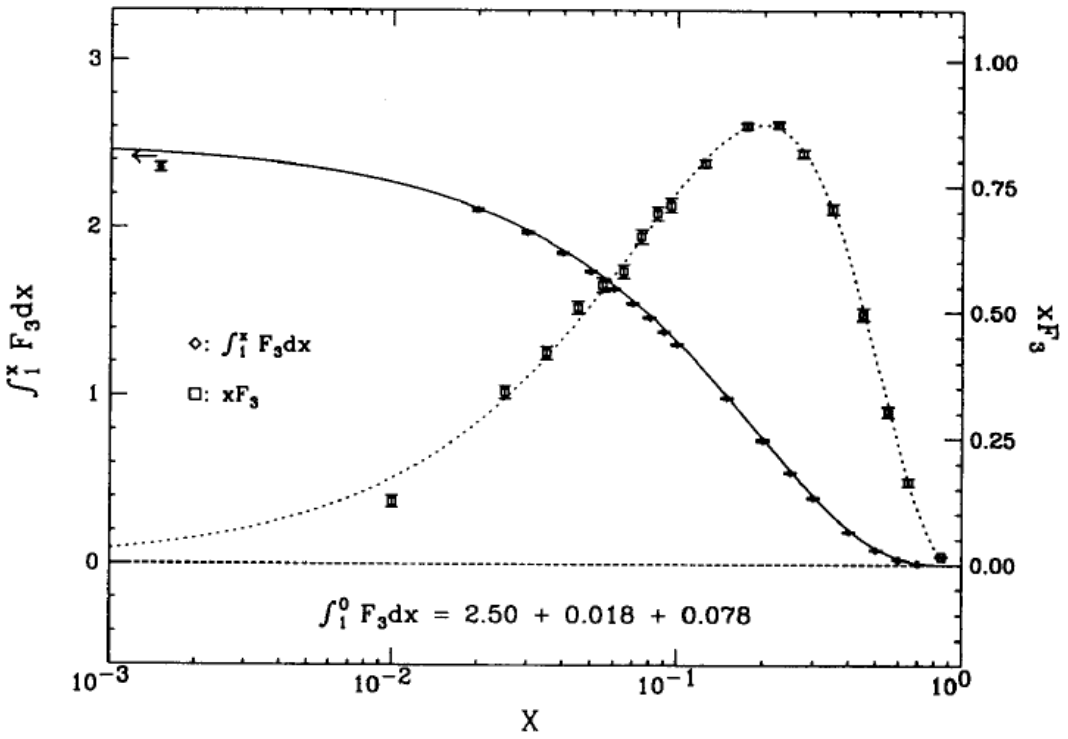

Figure 2.6: CCFR measurements of GLS sum rule as a function of x[67].

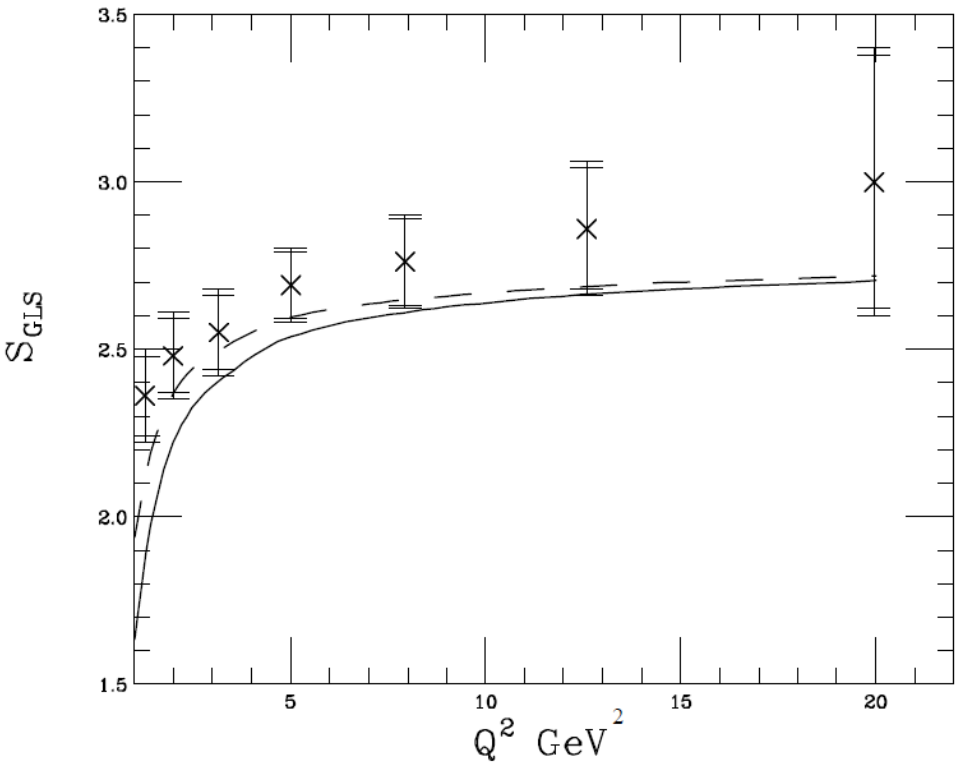

Figure 2.7: CCFR measurements of GLS sum rule as a function of Q^2[67]

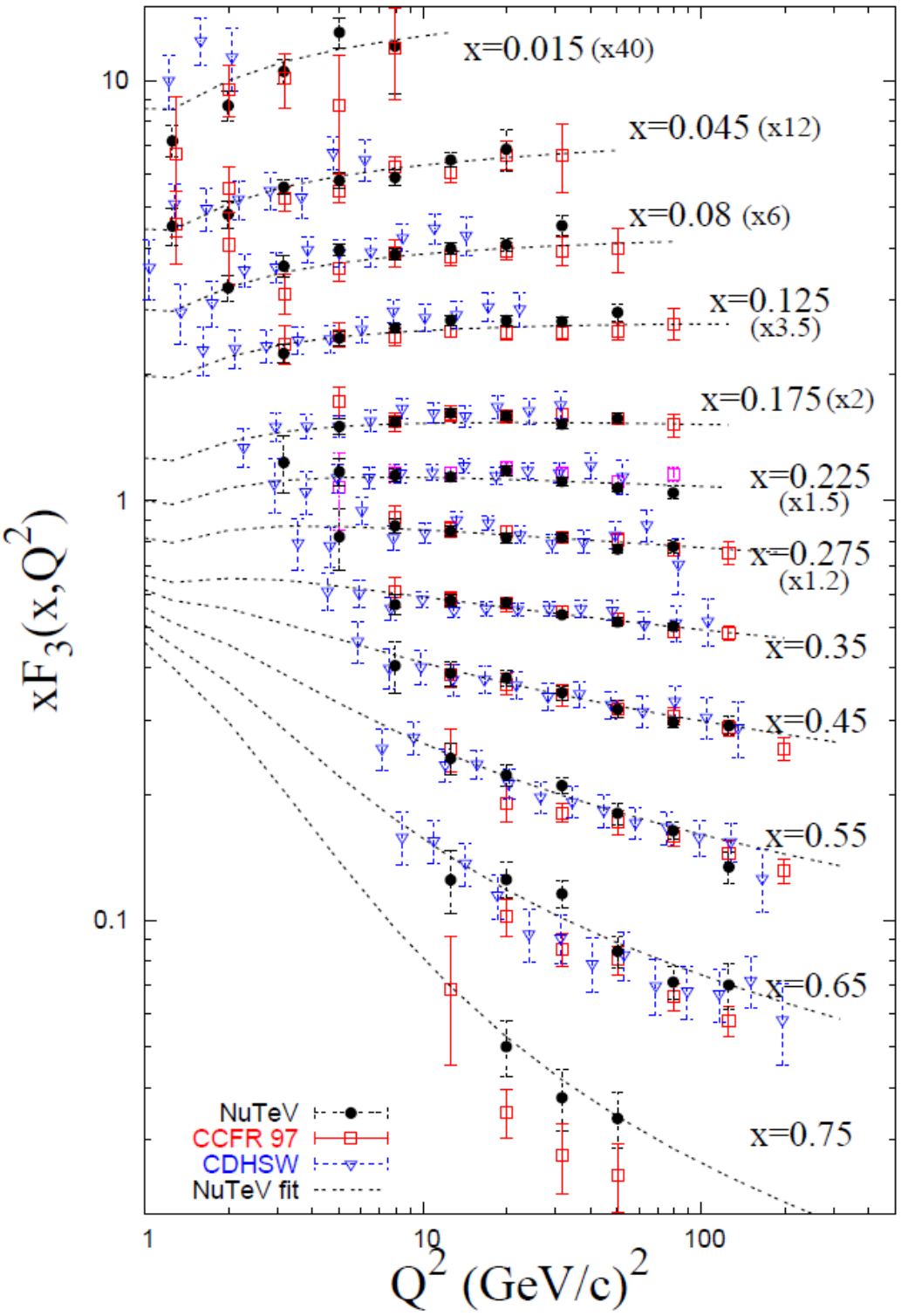

Figure 2.8: xF_3 structure function measured by NuTeV[68], CCFR[66] and CDHSW[69].

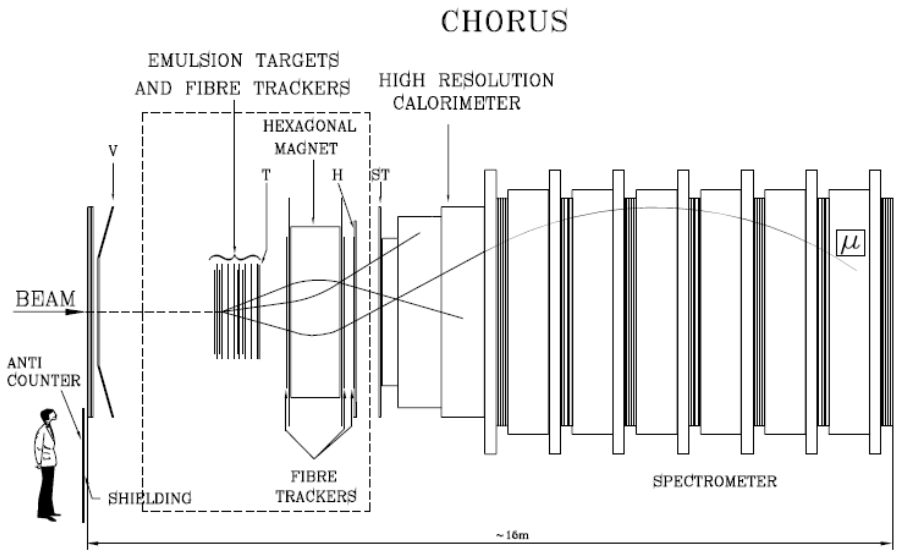

Figure 2.9: Schematic diagram of the CHORUS detector.

The NuTeV experiment took data during the 1996-97 fixed-target run at Fermilab. The main goal of NuTeV was the precise determination of $sin^2\Theta_W$. NuTeV's sign selected quadrupole train (SSQT) beamline was designed to select the sign of the pions and the kaons. The result was high purity separate ν_μ and $\bar{\nu}_\mu$ beams. Continuous calibration beam, running concurrently with the neutrino beam, illuminated the NuTeV detector with muons, electrons and pions. This allowed understanding of the muon and the hadron energy scales to precisions of 0.43% and 0.7% respectively. The NuTeV experiment has obtained a unique high statistics sample of neutrino and anti-neutrino interactions using its high-energy sign-selected beam. This measurement has significantly improved systematic precision as a consequence of more precise understanding of hadron and muon energy scales.(See [68, 81] for more details)

The $xF_3(x, Q^2)$ structure function determined from the linear combination of the neutrino and anti-neutrino differential cross sections measured in NuTeV [68] is shown in Fig. 2.8 along with previous measurements from CCFR and CDHSW.

2.2.4 CHORUS

The CERN Hybrid Oscillation Research ApparatUS (CHORUS)[82] is an experiment for differential measurements of neutrino induced Charged Current DIS and to study the Z/A dependence of the total Charged Current cross section[83].

CHORUSs detector (shown in Fig. 2.9) consisted of two parts (See [82, 84] for more details): a lead-scintillator-fiber calorimeter used as an active target and a magnetizediron muon spectrometer. The experiment utilised proton beam from the

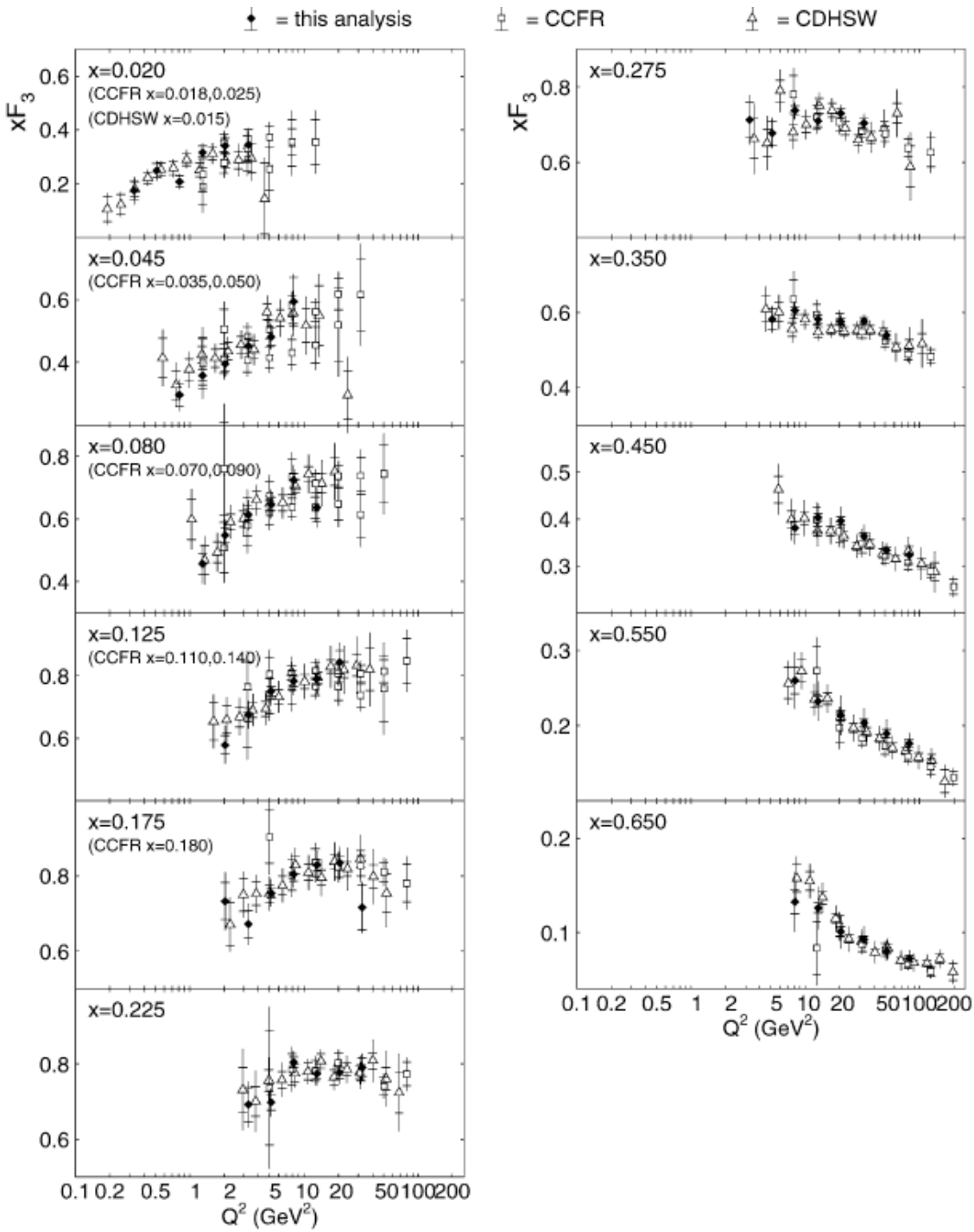

Figure 2.10: CHORUS measurements of xF_3 structure function along with CCFR and CDHSW data.

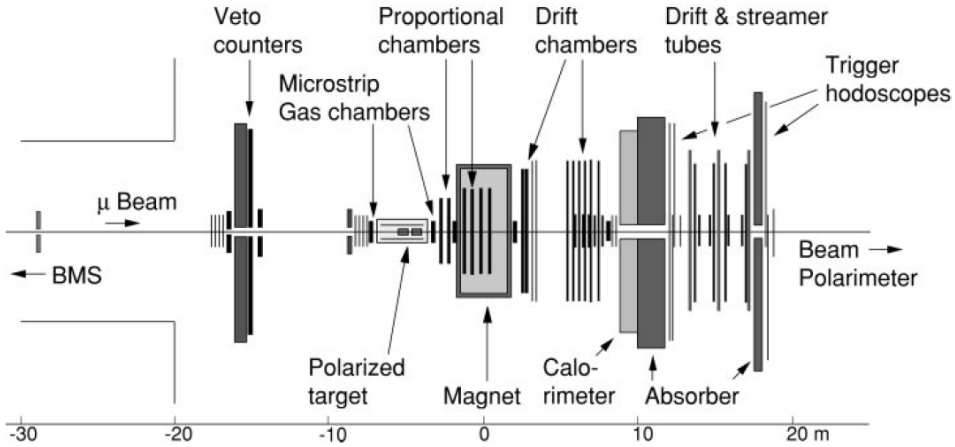

Figure 2.11: Schematic diagram of the Spin Muon Collaboration spectrometer.

Super Proton Synchrotron (SPS) with $450 GeV/c$ momentum interact in the target producing pion and kaons, which are focused by two pulsed toroidal magnets called horns. The decay of the mesons results in a wide-band neutrino beam, which was utilised in CHORUS experiment to take data in 1995-1998 using the lead-scintillator calorimeter as an active target[70].

The results for xF_3 structure function extracted from the CHORUS measurement[70] of differential cross sections within the kinematical range $0.02 \leq x \leq 0.65$ and in the $0.2 \leq Q^2 \leq 82 GeV^2$ are shown in Fig. 2.10 along with the results of CCFR[66] and CDHSW[69] collaborations. We have utilised these results in our phenomenological analysis performed in this thesis.

2.2.5 CDHSW

The CERN-Dortumund-Heidelberg-Saclay-Warsaw (CDHSW) experiment[85,86] measured the total neutrino cross section using 100-, 160-, and 200-GeV narrow-band neutrino beams and performed precision electroweak and structure function measurements with a wideband beam during 1982-1984. CDHSW experimental apparatus[85] consisted of a big iron toroid, interspersed with scintillator to act as a calorimeter, magnetised and equipped with drift chambers to measure the energy of the scattered muon in charged current interactions. This experiment used the CERN neutrino beam in the "wide band" mode which allowed a considerable increase in neutrino intensity and thus in statistics.

The xF_3 structure function data that is used in our analysis are depicted in Fig. 2.8 and 2.10 along with CCFR, NuTeV and CHORUS data.

2.2.6 SMC

The Spin Muon Collaboration(SMC) is a third reincarnation of the EMC detector designed to measure the spin-dependent asymmetries of longitudinally polarized muons scattering from polarized targets. SMC began operation in 1991.

The SMC experimental setup was similar to that used by the EMC collaboration. It used the same beam as the EMC experiment; the beam optics were improved to provide a smaller beam spot at the target location. A beam polarimeter, downstream of the scattered-muon spectrometer, allowed measurement of the beam polarization either by muon scattering on polarized electrons in a magnetized foil[87] or by measuring the Michel spectrum of positrons from C decay [87, 88].

The polarized target design[89] was based on the same principles as the EMC target. It consists of two $60cm$-long cylindric target cells separated by a $30cm$ gap. For most of the data taking solid butanol and deuterated butanol, respectively, were used as target material; however solid ammonia was used for the last data-taking period in 1996.

The SMC spectrometer (see Fig. 2.11) is based on a conventional wide-aperture dipole magnet operated with a bending power of 4.4 Tm at a beam energy of 190 GeV. A large array of multiwire proportional chambers installed before, inside, and behind the magnet is utilised to measure the scattered muons and in a $2m$-thick iron absorber the debris of hadrons produced in deep inelastic interactions is stopped. In addition another spectrometer consisting of multiwire proportional chambers, streamer tubes, and drift tubes is used in order to identify the scattered muons by observing tracks. The muon trigger is provided by predefined coincidence patterns between three arrays of plastic scintillation counters, two of which are installed behind the hadron absorber.

SMC measurements for g_1^{NS} and BSR are shown in Figs. 2.13 and 2.14 respectively along with other measurements.

2.2.7 COMPASS

COMPASS[90] is a dedicated polarized deep inelastic muon-scattering experiment installed at CERN SPS and uses a $160-200GeV$ longitudinally polarized muon beam with a polarization of about 80% and an intensity of $2 \times 10^8 + /spill$. The polarized deuteron (6^LiD) target consists of an upstream and a downstream cell with opposite polarization. The particles produced in the interaction are detected behind the target in a two-stage spectrometer with high momentum resolution and high rate capability.

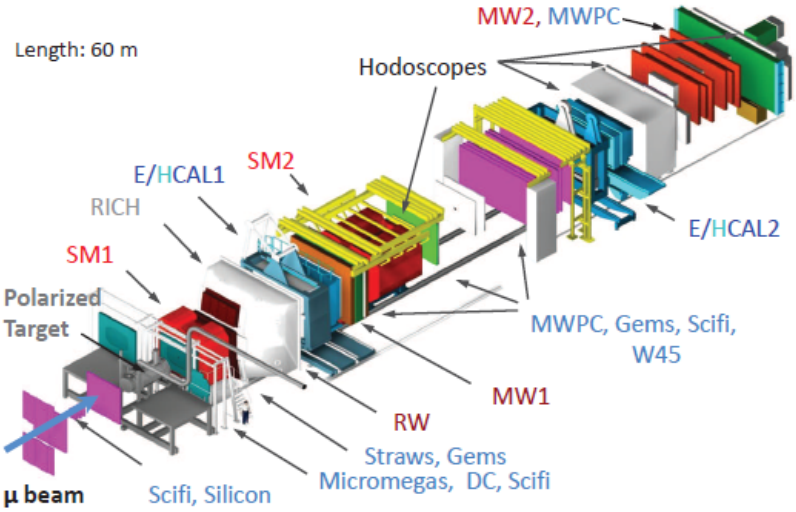

Figure 2.12: Schematic diagram of the COMPASS spectrometer.

--

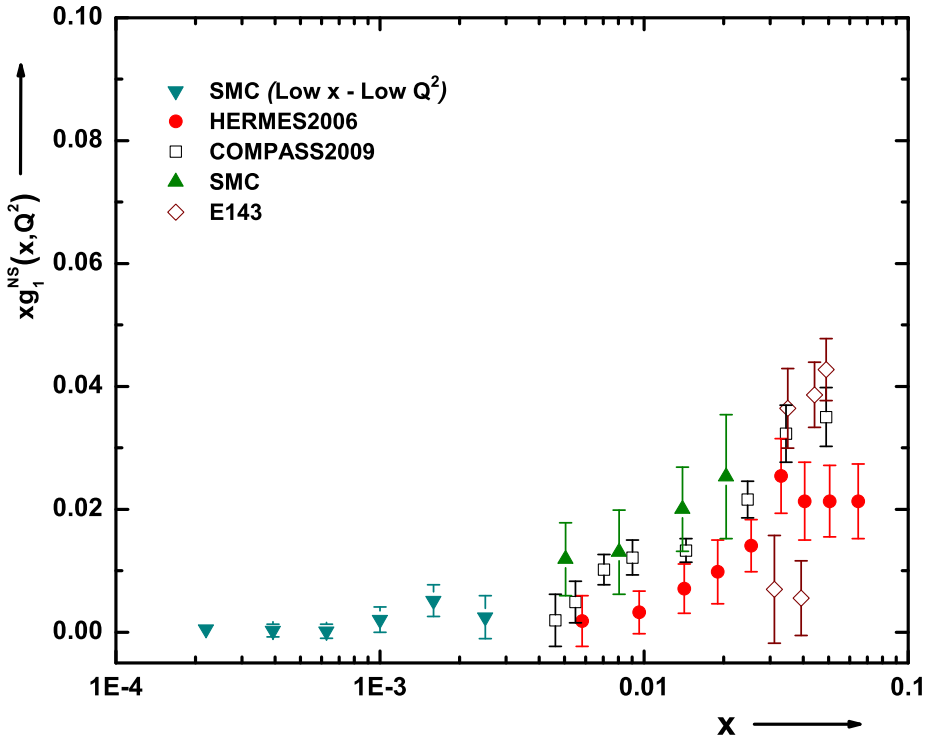

Figure 2.13: Spin-dependent non-singlet structure function xg_1^{NS}, measured by various experimental collaborations.

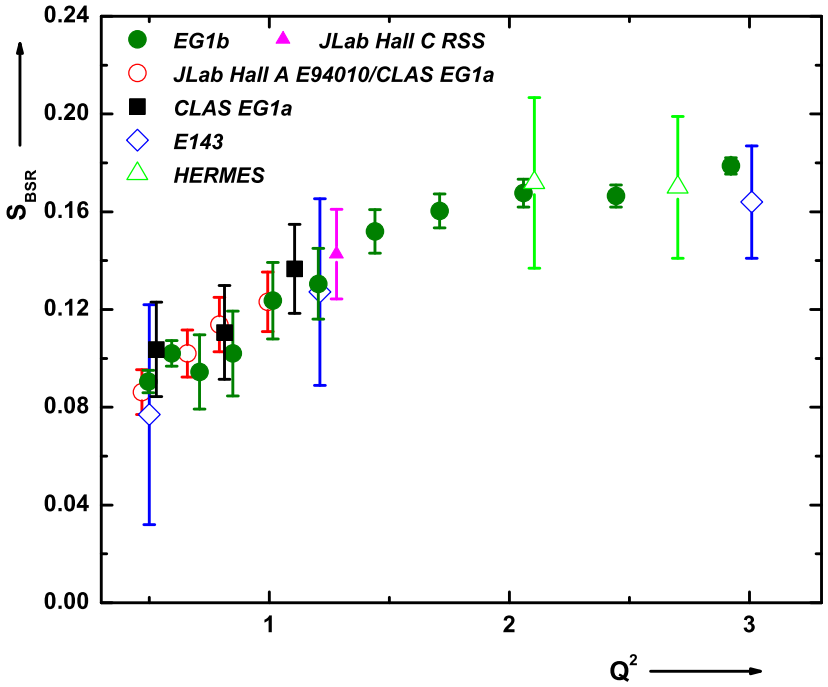

Figure 2.14: Experimental results for Bjorken Sum Rule.(Q^2's are taken in the unit of GeV^2).

COMPASS took data from 2002 to 2004, accumulating an integrated luminosity of $\sim 4.6 fb^{-1}$.

The results taken from [71] for spin dependent non-singlet structure function g_1^{NS} and the corresponding Bjorken Sum Rule(BSR) are shown in Figs. 2.13 and 2.14 respectively along with other measurements.

2.2.8 HERMES

The HERMES experiment[91] at DESY was designed to the disentangle the contributions from the different quark flavours to the nucleons spin in semi inclusive deep inelastic scattering reactions. In such reactions, hadrons are detected in coincidence with the scattered lepton. The flavour of the quark probed in the scattering process can be deduced from the charge and the type of the observed hadron in a statistical analysis. The HERMES experiment employed an innovative technique for the polarized target, which is very different from all other polarized DIS experiments. Gas targets of pure nuclear-polarized atoms of hydrogen or deuterium were used, which permit essentially background-free measurements from highly polarized nucleons with

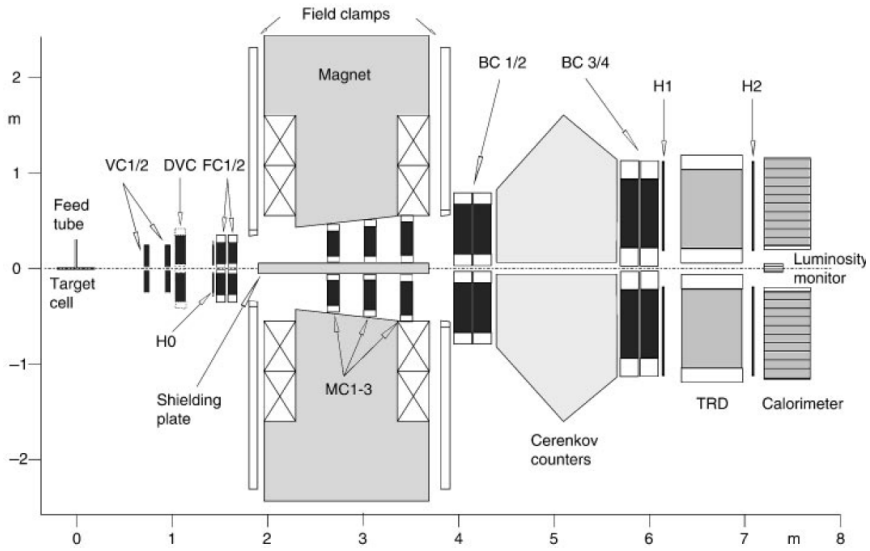

Figure 2.15: Schematic diagram of the HERMES spectrometer.

little or no dilution of the signal from unpolarized nucleons in the target. This choice eliminates one of the main systematic sources in polarized DIS, the uncertainty in the determination of the dilution factor.

The spectrometer (Fig. 2.15) consists of a large magnet followed by a detector package. The magnet bends charged particles produced in the interactions at the target, and the detectors are used for particle identification and momentum determination. The detector package in HERMES relies on a threshold Cerenkov counter and transition radiation detector for particle identification and tracking chambers with a rear lead-glass calorimeter for momentum and energy determination. Recently, a Cerenkov ring imaging detector has been installed at HERMES to tag hadrons and, in particular, kaons produced in the DIS interactions. The beam operates in a continuous mode, so it is straightforward to tag final state particles for studies of semi-inclusive scattering. The strength of the HERMES program lies in its clean identification of the interaction and complete event reconstruction using pure polarized gas targets.

HERMES measurements of g_1^{NS} and BSR, which are used in our analysis are included in Fig.2.13 and 2.14.

2.2.9 JLab Experiments

Thomas Jefferson National Accelerator Facility(TJNAF), commonly called Jafferson Lab or JLab, is a U.S. National laboratory located in Virginia. The experiments at Jefferson Lab utilized the highest polarization electron beams (85%) with energy ranging from 0.8 GeV close to 6 GeV. The technologies of polarizing beam and target

follow those pioneered and further developed at SLAC. The beam was provided by the Continuous Electron Beam Accelerator Facility (CEBAF)[92], which used polarized electron guns based on a "superlattice of a thin gallium arsenide (GaAs) layer on top of GaAs-phosphide bulk matter illuminated by circularly polarized photons from high intensity lasers [93]. Subsequently, the polarized electrons passed up to five times the two linear accelerators based on superconducting radio frequency technology and connected by two recirculation arcs. The spin direction of the electrons was manipulated using the crossed electric and magnetic fields of Wien filters, which allow for rapid spin rotation. Their direction was inverted every about 30 ms. Beam polarimetry was employed at several stages of the acceleration process. CEBAF delivered polarized beams simultaneously to the three experimental halls (Hall A, B and C) with the option to independently dial the energy and intensity. Typical beam intensities ranged from a few nA in Hall B to over $100A$ in the other two halls[94].

Longitudinal polarized solid state ammonia (NH_3) targets for the proton and ND_3 for the deuteron were employed at Hall B[95]. Hall A used a polarized ^3He target. The target polarization was measured by both the NMR technique of adiabatic fast passage and a technique based on electron paramagnetic resonance[96]. Average target polarizations of about 55% were obtained. Hall A and C were both instrumented with small acceptance but high resolution spectrometers that could cope with the highest beam intensities but measured at fixed scattering angles. These spectrometers are equipped for high resolution tracking, precise time-of-flight measurements and lepton/hadron separation[97].

JLab measurements of BSR we have used in the phenomenological analysis of our BSR results are depicted in Fig. 2.14 along with other measurements.

2.3 Parameterizations and Results

Parton distribution functions are determined from fits of perturbative QCD calculations, based on the DGLAP evolution equations, to various sets of experimental data. These fits are regularly updated to account for new experimental input and theoretical developments. Modern pdf's extracted from global analyses of data from DIS and hadronic processes are provided by several groups. For purposes of comparison in this thesis we present a brief discussion on the parameterizations MRST[104–106] and MSTW[107], CTEQ[98], GRV[99, 100]and NNPDF[101–103].

2.3.1 MRST and MSTW2008

Martin-Roberts-Stirling-Thorne(MRST)[104–106] parametrization has the following functional behaviour

$$xf(x,Q_0^2) = A_0 x^{\alpha}(1-x)^{\beta}(1+\delta x^{\gamma}+\eta x), \tag{2.1}$$

parton	A_0	α	β	γ	δ	η
$d_v(x,Q^2)$	0.040	0.27	3.88	52.73	0.5	30.65
$d_v(x,Q^2$	0.158	0.25	3.33	5.61	0.5	55.49

Table 2.2: Parameters characterizing the MRST2001[104] NLO parton distribution functions at $Q_0^2 = 1GeV^2$ defined by Eq. (2.1).

and the Parameters characterizing the MRST2001 NLO parton distribution functions at $Q_0^2 = 1GeV^2$ are listed in Table 2.3. With this parametrization, they have been predicting the parton distribution functions including several data set from H1, Zeus, BCDMS, SLAC, FNAL E665, CCFR, Drell-Yan etc., since 2002. MRST2002[104] and MRST2003[105] were improved in MRST2004[106] by including the new HERA data at moderate values of x and high Q^2. Also in MRST2004, full NNLO splitting functions were used. Recently published MSTW[107] parametrization represents an update of MRST. This update has a number of new theoretical features aimed at the NNLO parametrization; e.g., NNLO corrections to the Drell-Yan data. This parametrization also includes NuTeV and CHORUS data, the CDFII data, HERA inclusive jet data as well as direct high-x data on the F_L structure function.

2.3.2 CTEQ

The most recent parametrizations from the Coordinated Theoretical-Experimental Project on QCD (CTEQ) is the CTEQ6 series[98]. CTEQ uses the following functional form of the distribution functions,

$$xf(x,Q_0^2) = A_0 x^{A_1}(1-x)^{A_2} e^{A_3 x}(1+e^{A_4}x)^{A_5}, \tag{2.2}$$

and the Parameters characterizing the CTEQ6M NLO parton distribution functions at $Q_0^2 = 1.69GeV^2$ are listed in Table 2.3. With this parametrization, they have been predicting different parton distribution functions. The CTEQ collaboration omits

parton	A_0	A_0	β	γ	δ	η
$d_v(x,Q_0^2)$	1.4473	0.616	4.9670	-0.8408	0.4031	3.00
$u_v(x,Q_0^2)$	1.7199	0.5526	2.9009	-2.3502	1.6123	1.5917
$g(x,Q_0^2)$	30.4571	0.5100	2.3823	4.3945	2.355	-3.000
$(\bar{u}+d)(x,Q_0^2)$	0.0616	-0.2990	7.7170	-0.5283	4.7539	0.6137
$s(x,Q_0^2)=\bar{s}(x,Q_0^2)$	0.0123	-0.2990	7.7170	-0.5283	4.7539	0.6137

Table 2.3: Parameters characterizing the CTEQ6M parton distribution functions at $Q_0^2 = 1.69GeV^2$ defined by Eq. (2.2).

data for $Q^2 \leq 4GeV^2$. In particular, CTEQ6 omits SLAC data as well as some high-Q^2 H1 data. CTEQ uses 10% systematic errors in quadrature with the statistical errors for the Drell-Yan data in comparison with 5% systematic errors assumed by MRST2002. CTEQ uses a starting scale of $Q_0^2 = 1.69GeV^2$.

2.3.3 GRV

The Gluck-Reya-Vogt(GRV) parton distribution functions were developed in a series of publications throughout the 1990s[99,100]. They are dynamical distributions, which are generated radiatively from valence-like inputs at a low resolution scale. The latest of this series makes use of the 1994-95 HERA data for $Q^2 \geq 2GeV^2$ as well as the SLAC, BCDMS, NMC and E665 data with $Q^2 \geq 4GeV^2$ and the simply extracted ratios F_2^n/F_2^p from the NMC, BCDMS and E665 experiments. This analysis takes into account the Drell-Yan data and the u_v/d_v ratios extracted from the CERN CDHSW and WA21 neutrino data.

The GRV parton distribution functions are parametrized as

$$xf(x,Q_0^2) = A_0 x^\alpha (1-x)^\beta (1+\delta\sqrt{x}+\eta x), \tag{2.3}$$

parton	A_0	α	β	δ	η
$d_v(x,Q_0^2)$	0.761	1.48	3.62	-1.8	9.5
$u_v(x,Q_0^2)$	1.239	0.48	2.72	-1.8	9.5
$x\Delta(x,Q_0^2)$	0.23	0.48	11.3	-12.0	50.9
$x(\bar{u}+d)(x,Q_0^2)$	1.52	0.15	9.1	-3.6	7.8
$xg(x,Q_0^2)=\bar{s}(x,Q_0^2)$	17.47	1.6	3.8	-	-

Table 2.4: Parameters characterizing the GRV98LO parton distribution functions at $Q_0^2 = 1.69GeV^2$ defined by Eq.(2.3).

parton	A_0	α	β	δ	η
$d_v(x,Q_0^2)$	0.394	1.43	4.09	-	18.2
$u_v(x,Q_0^2)$	0.632	0.43	3.09	-	18.2
$x\Delta(x,Q_0^2)$	0.20	0.43	12.4	-13.3	60.0
$x(\bar{u}+\bar{d})(x,Q_0^2)$	1.24	0.20	8.5	-2.3	5.7
$xg(x,Q_0^2)=\bar{s}(x,Q_0^2)$	20.80	1.6	4.1	-	-

Table 2.5: Parameters characterizing the GRV98NLO parton distribution functions at $Q_0^2 = 1.69GeV^2$ defined by Eq.(2.3).

and the parameters for GRV98LO and GRV98NLO are listed in tables 2.4 and 2.5 respectively. These distributions are characterized by a relatively low starting scale for evolution: LO, $Q_0 = 0.5GeV$; and NLO, $Q_0 = 0.63GeV$.

2.3.4 NNPDF

The consideration of a specific parametrization with large number of parameters is potentially a source of bias, i.e. systematic error which is very difficult to control. Furthermore, when a parametrization is fitted to the data, it is very hard to obtain a determination not only of the best fitting parameters, but also of their errors. Therefore, explorations of the possibility of obtaining accurate solutions of DGLAP evolution equations without an initial input or with initial input, consisting of less number of parameters are always interesting. NNPDF method is one of the most interesting methods which does not require to assume a functional form and it is largely bias free[101–103]. NNPDF uses neural networks to parameterise the densities. The formalism is described in [102] and references therein. Neural networks are just another functional form, that generalises parameterisations like $xf(x) = \sum_n \alpha_n P_n(x)$ based on interpolation polynomials $P_n(x)$. They allow non-linear dependencies of the function on the fitted parameters α_n.

The analysis presented in [102] fits the gluon density together with the six densities for light quarks and anti-quarks u, $\bar{u}$, d, $\bar{d}$, s, $\bar{s}$. The neural networks chosen to parameterise these densities have 37 free parameters each. Hence, the resulting parameterisation has a total of $7 \times 37 = 259$ free parameters, which is much larger than the number of free parameters, O(25), which are fitted in QCD analyses based on a standard functional form like Eq. (2.3). The use of such a flexible parameterisation scheme considerably reduces any parameterisation bias. □□